

# Multi-rate switched capacitor filter design with aggressive sampling-rates: filterX in action

Chris Ouslis, Martin Snelgrove Adel S. Sedra

Dept. of Electrical Engineering, University of Toronto  
Toronto, Ontario, CANADA, M5S 1A4  
Tel: 416-978-2799 Fax: 416-978-7423  
e-mail: ouslis@macedonia.eecg.toronto.edu

## Abstract

Multi-rate switched capacitor (SC) filter design is an effective means of minimising silicon area for bandpass systems. The theory derived allows designs to achieve maximal area savings by employing sampling-rates approaching the minimum allowed by sampling theory. Designing filters to simultaneously operate at different sampling rates can require numerical optimisation to correct for the effects of multi-rate operation. **filterX**, the computer aided filter design tool was employed to design a CCITT V.22 high-band modem filter as a test of the derived design methodology. The result was an improvement of the uncorrected multi-rate filter which had exceeded passband tolerances, to one which was within tolerances. The multi-rate filter, operating at sampling rates of 128kHz and 8kHz required 70% less capacitor area than the equivalent single-rate filter operating at a sampling rate of 128kHz.

## 1. Introduction

SC filter design is a very mature field which still has challenging engineering avenues to explore. One example of these involves the design of multi-rate filters at sampling-frequencies approaching the minimum allowed by the sampling theorem [1]. Multi-rate, switched-capacitor filters employ a number of filter sections, operating at different clock rates, cascaded to produce a complete filter response. Many diverse applications employing various multi-rate techniques, from polyphase filters, decimators, and interpolators [2] [3], to multi-rate, adaptive, digital-filter concepts [4], provide many opportunities to apply new design approaches.

One of the advantages of multi-rate filtering is that the capacitance spread in wideband bandpass filters can be reduced. With high clocking rates typically found in switched-capacitor circuits, large capacitance ratios are required for filter sections with low frequency poles and/or zeros. Under certain conditions, the highpass section can be clocked at a lower rate than the lowpass section. The difference in sampling rates is limited by the stopband edge of the lowpass section which acts as the anti-aliasing filter for the following highpass section. The savings realised results from the lower clock rate used for the low-frequency poles and zeros of the highpass sections; typically, large capacitor ratios are necessary due to the large difference between the clock rate and the pole and zero frequencies. Lowering the clock rate achieves an area savings proportional to the ratio of clock rates of the lowpass sections (the original rate) and the highpass sections (at the reduced rate).

The inherent difficulty in the design process is due to the complexity of dealing with a shaped passband created by filter sections operating at different sampling frequencies. In designing a shaped passband filter, it is necessary to work with the transfer function at a single sampling rate, the higher sampling frequency, then to separate the transfer function into lowpass and highpass sections; the highpass section is then transformed to the lower sampling rate for implementation. When the sampling frequency of the highpass section is sufficiently large, the effects of the transformation are virtually negligible. For designs which maximise the benefit of multi-rate sampling to achieve the greatest area savings,

those operating with sampling frequencies near the theoretical minimum (twice the maximum frequency of interest), the effect of the low sampling rate can be significant. This is particularly apparent in shaped passband filters.

The problem is then to develop a technique which provides designers with a means of exactly determining the correct rational function for any reasonable sampling rate. The resulting cascade of the individual filter sections should then meet the desired system specifications. Designers will then be able to achieve the greatest benefit in area savings by utilising the lowest possible sampling-rate for any given situation.

## 2. Theory

For sampled data systems, real frequencies are represented by traversing the unit-circle. When evaluating a system which operates at two sampling rates, a multi-rate system, real frequencies no longer coincide on one unit circle. Each filter is represented by a unit circle and its respective sampling rate. To evaluate multi-rate systems, one rate must be chosen as the base upon which to work; real frequencies for both systems will be represented on one unit-circle. For this purpose, the unit circle and frequency representations of the higher sampling frequency are used. To illustrate, Figure 1 shows a system at a sampling rate  $f_s=F$  and a second system at a sampling rate of  $f_s=2F$ .

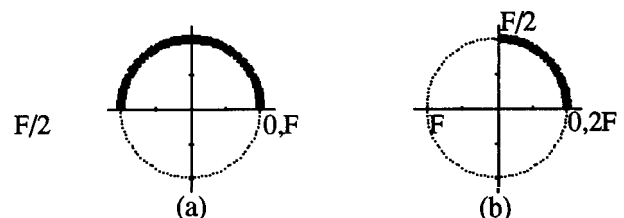


**Figure 1.** a) System at a sampling rate of  $f_s=F$ . b) System at a sampling rate of  $f_s=2F$ . Darkened regions are spans of the same frequency range at the two sampling rates.

At the given sampling rates, a traversal of the upper-half unit-circle for the lower sampling rate  $F$  (Figure 1a) occupies only the upper-right quadrant of the unit-circle at the higher sampling rate  $2F$  (Figure 1b). By analogy, the unit-circle of Figure 1a) would then be traversed twice to represent the system's response for the unit-circle in Figure 1 b).

The result of this mapping of the unit-circle for the lower sampling rate system into a fraction of the unit-circle at the higher sampling rate is that the poles and zeros of the rational functions are mapped into a smaller region ( $1/N$  of the unit circle) of the  $z$ -plane at the higher sampling rate ( $N$  times higher). In fact, the poles and zeros are then replicated until the entire frequency range, up to the sampling rate, is covered. Based on a ratio of sampling rates of 2, Figure 2 shows how poles and zeros would be transformed from the lower sampling rate to the higher.

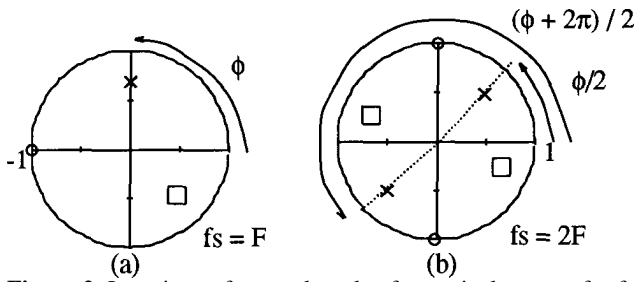


**Figure 2.** Locations of example poles for equivalent transfer functions at different sampling rates. a) Poles of a rational function with sampling rate  $f_s=F$ . b) Poles of (a) transformed into the  $z$ -plane where the sampling ratio is  $f_s=2F$ .

All  $N$ ,  $N$ th roots are determined from the transformation to a plane in which the sampling ratio is  $N$  times greater. This transformation, shown as equation 1, preserves the transfer function characteristics of the rational function over the original frequency range and preserves the effects of aliasing beyond the original Nyquist rate.

$$\begin{aligned} &\text{for ( each pole and zero )} \\ &\text{for ( } i = 0 ; i < N ; i = i + 1 \text{ )} \\ &\text{new} = |\text{poleorzero}| \frac{1}{N} e^{j \frac{\text{angle}(\text{root}) + i * 2\pi}{N}} \end{aligned} \quad (1)$$

The  $N$ th roots of each of the poles and zeros are taken to transform the lower sampling frequency transfer function to an equivalent one at a higher rate. The transformation can be thought of as substituting each of the unit delays in the lower sampling rate system with  $N$  unit delays at the higher sampling rate; now, operating the system at the higher sampling rate yields the same response (except for an error in the gain). The net effect on the rational function is to transform each pole and zero into the  $N$ ,  $N$ th roots mentioned previously. Figure 3. illustrates these ideas.

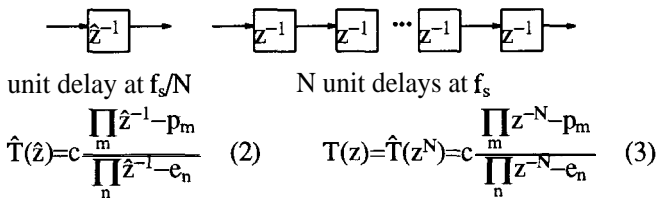


**Figure 3.** Symbolic representations of transforming a system from a sampling frequency of  $f_s/N$  to  $f_s$  and related effects for the system transfer function. Note that the order of  $T(z)$  increases by a factor  $N$ .

Now both systems can be expressed from a common perspective: the higher sampling rate. The operation of the complete system can be determined by cascading the sections, which is equivalent to multiplying the two rational functions. The result contains the  $N$  replicas of the lower sampling rate system and the poles and zeros of the higher rate system all in the  $z$ -plane.

It should be noted that the subject of aliasing has not been dealt with, but is a factor which should not be ignored. Common situations consist of a lowpass system sampled at the higher rate followed by a highpass system sampled at the lower rate. Since the second stage of this system is operating at  $f_s/N$ , aliasing will occur for any frequencies beyond  $f_s/2N$ . Thus, the lowpass system will act as the anti-aliasing filter for the lower sampling-rate, highpass system. This implies that the stopband characteristics of the lowpass will limit the factor of sampling rate reduction. Furthermore, the degree of attenuation in the lowpass stopband will determine, along with the input spectrum, the degree of error due to aliasing that the highpass section will experience. In other words, because the preceding lowpass section is the anti-aliasing stage for

the following highpass sections, it must meet an anti-aliasing specification in addition to its original specifications. For some system specifications, the designer must determine if additional stopband attenuation will be required from the lowpass filter to obtain proper operation of the highpass filter. In a switched-capacitor application, this may be a question of area savings: determining the net effect of increasing the lowpass order while decreasing the capacitor ratios of the highpass system.

### 3. Design Methodologies

Two basic methodologies exist for multi-rate filter design. The first is a simple technique which can be applied to filters with flat passbands; the non-ideal effects resulting from aggressive clocking techniques are virtually negligible in these filters. Applications for filters with flat passbands are generally historical, or appropriate for cookbook design techniques. A thorough technique is required to deal with challenging specifications faced by today's designers. The second approach accurately quantifies the filter response under the conditions of an aggressive sampling rate, thus allowing numerical optimisation to correct for any undesired effects, even for shaped passbands.

The first method can be accomplished by two differing approaches. Since the desired passband is flat, the design can be separated into two independent filters, each to be designed at its given sampling rate. When the designs are complete, their cascade will meet passband specifications provided the individual passband ripple values summed to the desired final value. The second design method is the same as that outline below for shaped passbands. The only difference being that no optimisation is required for the traditional flat passband. The final response should be negligibly different from that originally designed at the higher sampling rate (if there are no effects due to the chosen sampling rate).

Shaped passband specifications are best dealt with by employing the second method, whereby the filter is designed at the higher sampling rate. Upon obtaining the complete filter, it is separated into lowpass and highpass sections. The lowpass section is left as is since its sampling rate is correct. The highpass section is then transformed to the equivalent lower sampling rate rational function, but is expressed at the higher sampling rate (2). This is done by replicating the roots (evenly spaced)  $N$  times around the unit circle. By referring to Figures 2 and 3, it should be evident that a rational function with these characteristics can be expressed as a rational function of lower order (by a factor  $N$ ) at a sampling rate  $N$  times lower. Two problems follow this transformation the first is that there is a gain error; the second is caused by the presence of the replicated poles and zeros which affect the resulting transfer function causing undesired effects in the passband – this can be corrected through optimisation.

The gain error is a result of the fact that the transformation is not exact in the calculation of the gain coefficient for the replicated function. A correction for the gain error can be applied by noting that the action of replicating the roots around the unit-circle is equivalent to taking the product of the original rational function's poles and zeros at the  $N$  roots of  $-1$  around the unit-circle.

$$T'_{HP}(z) = c \prod_{i=0}^{N-1} T_{HP}(ze^{j \frac{2\pi i}{N}}) \quad (4)$$

We want  $T'_{HP}(1) = T_{HP}(1)$

$$T'_{HP}(1) = c \prod_{i=0}^{N-1} T_{HP}(e^{j \frac{2\pi i}{N}}) \quad (5)$$

$$= c T_{HP}(1) \prod_{i=1}^{N-1} T_{HP}(e^{j \frac{2\pi i}{N}}) \quad (6)$$

hence,

$$c = \frac{1}{\prod_{i=1}^{N-1} T_{HP}(e^{j \frac{2\pi i}{N}})} \quad (7)$$

This guarantees that the transformed rational function will exhibit the same gain as the original at  $z=1$ .

We now have the lowpass rational function expressed at its sampling rate and an equivalent highpass rational function expressed at the same sampling rate. Using a numerical optimiser, we can now alter the transfer function of the lowpass filter to accommodate the effects of the multi-rate operation of the two filter sections. The final lowpass filter can then be directly implemented as a switched capacitor circuit. The highpass rational function can then be transformed into its lower sampling rate equivalent function. The final rational function,  $T'$ , consists of lowpass and highpass functions.

$$T' = c_T \frac{\prod_{i=1}^{m_{HP}+m_{LP}} z^{-1}-p_i}{\prod_{i=1}^{n_{HP}+n_{LP}} z^{-1}-e_i} = c_T T'_{HP} T_{LP} \quad (8)$$

Since the poles and zeros of the highpass rational function exhibit  $N$  symmetry around the unit circle, we can express the poles and zeros as the  $N$ th power roots,

$$\begin{aligned} &= c_T \frac{\prod_{i=1}^{m_{HP}/N} z^{-N}-p_{i,HP}^N \prod_{i=1}^{m_{LP}} z^{-1}-p_{i,LP}}{\prod_{i=1}^{n_{HP}/N} z^{-N}-e_{i,HP}^N \prod_{i=1}^{n_{LP}} z^{-1}-e_{i,LP}} \\ &= c_T T'_{HP} T_{LP} \end{aligned} \quad (9)$$

$$= c_T T'_{HP} T_{LP} \quad (10)$$

where  $T_{LP}$  is the original lowpass rational function. Because of the symmetry of  $T'_{HP}$ , we can now transform it to a lower sampling rate.

$$\hat{T}_{HP}(\hat{z}) = T'_{HP}(z) |_{(z=z^N)} \quad (11)$$

$$= \frac{\prod_{i=1}^{m_{HP}/N} \hat{z}-p_{i,HP}^N}{\prod_{i=1}^{n_{HP}/N} \hat{z}-e_{i,HP}^N} \quad (12)$$

This final transformation to  $\hat{T}_{HP}$  has a factor of  $N$  fewer poles and zeros than  $T'_{HP}$  and has relocated each pole and zero at a sampling rate  $f_s/N$  as compared to the original sampling rate of  $f_s$ .  $\hat{T}_{HP}$  can now be implemented as a switched-capacitor circuit at its lower clocking speed.

#### 4. Design Example

To apply the theory, a shaped-passband specification was chosen. The CCITT V.22 specification for 1200 baud modems provided a challenging problem, from which the "high band" filter was chosen. This specification is particularly interesting due to its sloping passband. Table 1 [5] lists some of the points adapted from the original specification. **filterX** was used to carry out all the necessary manipulations, and optimisation of the rational functions. All the operations were written in **filterX** code, and no additional coding was required in any other programming language.

It was determined that a second-order lowpass filter coupled with a fourth order highpass filter would be sufficient to meet the specifications. A clocking speed of 128kHz was chosen for the lowpass filtering section. It was decided that, based on the specification, the highpass section would be operated at a sampling rate of 8kHz although there is a possibility of abasing distortion for input spectra with significant signal power above 4kHz. This is a result of the upper stopband requiring only 20dB of attenuation while the lower stopband requires 50dB. In a situation such as this, it may be pragmatic to increase the order of the lowpass filter to

**Table 1.** Filter gain specifications

freq (Hz)	gain(dB)	
	min	max
800		-50
1600		-50
2000	-1.5	0.0
2800	0.0	1.5
3200		-10
3500		-20

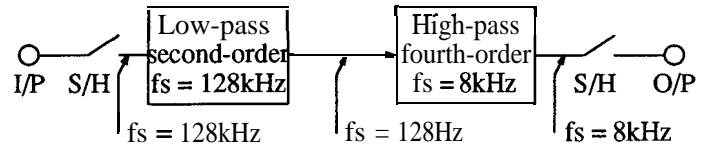


**Figure 4.** A block diagram of the band-pass system, indicating the location of the sample-and-hold circuits along with the sampling rates at various locations in the system.

four, and thus provide increased attenuation against abasing problems for the lower sampling rate section. Since it was a telecom application, it was assumed that there would likely be little, if any, power at, or above, 4kHz; the choice of a sampling rate of 8kHz would then yield maximal area savings, although the effects of the aggressive sampling rate chosen would have to be dealt with. The resulting configuration of the system is illustrated in Figure 4.

As an example of the effect caused by the limitations of a low sampling rate, the responses of the high-pass filters (one operating at  $f_s=128$ kHz, while the other has been transformed, following the steps given in the text, to  $f_s=8$ kHz) are plotted in Figure 5. It should be noted that the effect is solely the result of the chosen sampling rate, and would be less pronounced for a higher sampling rate – in fact, there is an insignificant gain error, and a negligible effect on the passband for  $f_s=16$ kHz. Figure 6 shows the complete transfer function of the final filter after optimisation. Figure 7 illustrates that the filter, before re-optimisation for multi-rate operation, had exceeded the allowed specification; comparing the passband region of Figure 5 and that of Figure 7, the source of the error in this region is obviously the effect of the high-pass response serving to emphasise the gain as frequency increases. By optimising the low-pass (second-order) section, the filter was corrected to within the allowed tolerances. Both are compared to an **ideal** filter designed to operate at 128kHz.

The change required of the low-pass section was minor, as is seen in Table 2 by the slight change in capacitor ratios. Table 2 lists the capacitor ratios and the number of required unit capacitors for each of the biquads. It can be seen that the capacitor ratios for the high-pass biquads change significantly for the lower sampling rate, which, in turn, yields a dramatic reduction in the overall area. By assigning a unit size capacitance to the smallest capacitor in the system, the number of unit capacitors required, and hence the area required, to realise the circuit can be quantified. From the totals of Table 2, an area savings of 70% is realised by a reduction of sampling rate by a factor of 16.

#### 5. Conclusions

A methodology to accurately design multi-rate switched-capacitor filters was derived. The theory applies equally well to systems employing aggressive sampling-rate reduction down to rates only slightly above the Nyquist criterion. The theory was applied using the **filterX** filter design package. Using **filterX**, a high-band V.22 modem filter was designed. The filter operates its lowpass section at 128kHz and its highpass section at 8kHz (significantly affecting the high-pass filter response). It was seen

Table 2. Biquad Capacitor Ratios

Single rate			Optimised multi-rate		
cap name	cap ratio	# of unit caps	cap name	cap ratio	# of unit caps
Low-pass biquad					
fs = 128kHz			fs = 128kHz		
C1	1.0	214	C1	1.0	36
C2	1.0	214	C2	1.0	36
K3C2	0.1215	26	K3C2	0.1214	4
K1C1	0.0281	6	<b>K1C1</b>	<b>0.0277</b>	<b>1</b>
K5C2	0.1359	29	K5C2	0.1368	5
K6C1	0.0822	18	K6C1	0.0865	3
K4C1	0.1359	29	K4C1	0.1368	5
High-pass biquad 1					
fs = 128kHz			fs = 8kHz		
C1	1.0	214	C1	1.0	36
c 2	1.0	214	C2	1.0	36
K3C2	0.4842	104	K3C2	0.4329	16
K1C1	0.0251	5	K1C1	0.3690	13
K5C2	0.0988	21	K5C2	1.3828	50
K6C1	0.0744	16	K6C1	0.0805	3
K4C1	0.0988	21	K4C 1	1.3828	50
High-pass biquad 2					
fs = 128kHz			fs = 8kHz		
C1	1.0	214	C1	1.0	36
c 2	1.0	214	C2	1.0	36
K3C2	0.4636	100	K3C2	0.2878	10
K5C2	<b>0.0036</b>	<b>21</b>	K5C2	<b>0.0709</b>	<b>53</b>
K6C1	0.1872	40	K6C1	0.2004	7
K4C1	0.1155	25	K4C1	1.4729	53
total		1750			491

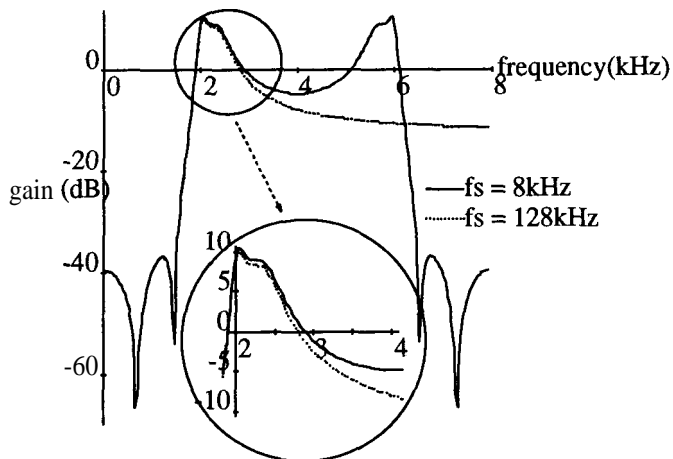


Figure 5. The high-pass sampled-data filter operating at sampling-rates of  $f_s=128\text{kHz}$ , and transformed to  $f_s=8\text{kHz}$ . Note the pronounced effect on the passband of the filter operating at (near the Nyquist frequency of  $f_s/2$ ). This artifact of the aggressive sampling rate chosen for the high-pass filter, must be dealt with in the design stage to ensure that the overall specifications of the system are met.

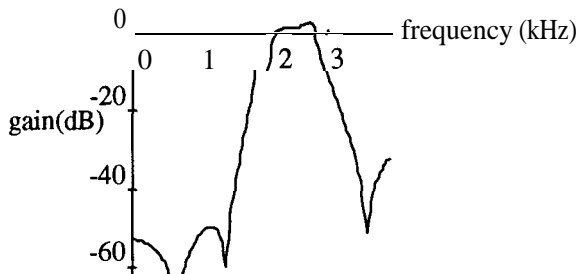


Figure 6. Transfer function of the final optimised multi-rate filter.

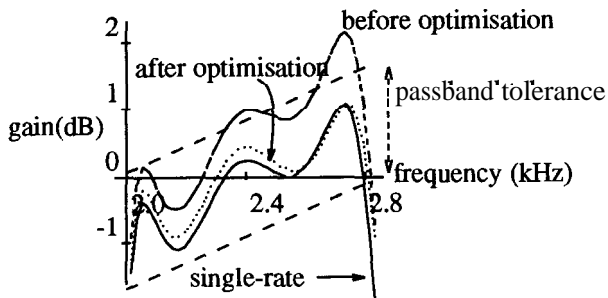


Figure 7. A passband detail of the filter showing a comparison of a single-rate filter operating at  $128\text{kHz}$ , the multi-rate uncorrected filter, and the multi-rate corrected filter. The specified tolerance band is also plotted for comparison.

that before correcting for multi-rate effects, the passband had exceeded the allowable tolerances. Optimising the rational functions using the derived multi-rate techniques yielded a filter which was within specifications. The multi-rate filter also exhibited a significant reduction (70%) in total capacitor area over the equivalent single-rate filter operating at only the higher sampling rate.

## 6. Acknowledgements

This work was supported in part by the Information Technology Research Centre (ITRC), a Province of Ontario funded Centre of Excellence, and by MicroNet, a federal Network of Centres of Excellence. Ken Martin's suggestions, and valuable comments are greatly appreciated by the authors.

Note that the smallest capacitor, that chosen as the unit capacitor, is emboldened for each system.

All capacitor values were generated from the transfer functions using filterX; capacitor names refer to [6].

## REFERENCES

- [1] R.E. Crochiere and L.R. Rabiner, *Multirate Digital Signal Processing*, Prentice-Hall, Inc., Englewood Cliffs, New Jersey 1983.
- [2] J.E. da Franca, "Nonrecursive Polyphase Switched-Capacitor Decimators and Interpolators," *IEEE Trans. Circuits Syst.*, vol. CAS-32, pp. 877-887, Sept. 1985.
- [3] J.E. da Franca and D.G. Haigh, "Design and Applications of Single-Path Frequency-Translated Switched-Capacitor Systems," *IEEE Trans. Circuits Syst.*, vol. CAS-35, pp. 394-408, April 1988.
- [4] J.J. Shynk "Frequency-Domain and Multirate Adaptive Filtering," *IEEE Signal Processing Magazine*, vol. 9, pp. 14-37, January 1992.
- [5] Mitel Semiconductor, *Microelectronics Data Book, Issue S. 1988*.
- [6] C. Ouslis, W.M. Snelgrove, and A.S. Sedra, *A filter designer's filter design aid: filterX* Singapore, Proceedings of the IEEE International Symposium on Circuits and Systems June 1991.